Molecular Systems Biology 7; Article number 542; doi:10.1038/msb.2011.76
Citation: ***Molecular Systems Biology* 7: 542**

www.molecularsystemsbiology.com

molecular systems biology

Carbohydrate-active enzymes exemplify entropic principles in metabolism

Önder Kartal[1,2,6], Sebastian Mahlow[2,6], Alexander Skupin[1,3,6] and Oliver Ebenhöh[4,5,6,*]

[1] Max Planck Institute of Molecular Plant Physiology, Potsdam, Germany, [2] Department of Plant Physiology, Institute of Biochemistry and Biology, University of Potsdam, Potsdam-Golm, Germany, [3] Luxembourg Centre for Systems Biomedicine, University of Luxembourg, Luxembourg, [4] Institute for Complex Systems and Mathematical Biology, Department of Physics, SUPA, University of Aberdeen, Aberdeen, UK and [5] Institute of Medical Sciences, University of Aberdeen, Aberdeen, UK
[6] These authors contributed equally to this work
* Corresponding author. Institute for Complex Systems and Mathematical Biology, Department of Physics, SUPA, University of Aberdeen, Meston Building, Meston Walk, Aberdeen AB24 3UE, UK. Tel.: +44 (0)1224 272520; Fax: +44 (0)1224 273105; E-mail: ebenhoeh@abdn.ac.uk

Received 14.6.11; accepted 9.9.11

Glycans comprise ubiquitous and essential biopolymers, which usually occur as highly diverse mixtures. The myriad different structures are generated by a limited number of carbohydrate-active enzymes (CAZymes), which are unusual in that they catalyze multiple reactions by being relatively unspecific with respect to substrate size. Existing experimental and theoretical descriptions of CAZyme-mediated reaction systems neither comprehensively explain observed action patterns nor suggest biological functions of polydisperse pools in metabolism. Here, we overcome these limitations with a novel theoretical description of this important class of biological systems in which the mixing entropy of polydisperse pools emerges as an important system variable. *In vitro* assays of three CAZymes essential for central carbon metabolism confirm the power of our approach to predict equilibrium distributions and non-equilibrium dynamics. A computational study of the turnover of the soluble heteroglycan pool exemplifies how entropy-driven reactions establish a metabolic buffer *in vivo* that attenuates fluctuations in carbohydrate availability. We argue that this interplay between energy- and entropy-driven processes represents an important regulatory design principle of metabolic systems.
Molecular Systems Biology **7**: 542; published online 25 October 2011; doi:10.1038/msb.2011.76
Subject Categories: metabolic and regulatory networks; plant biology; cellular metabolism
Keywords: energy metabolism; entropic enzymes; glycobiology; metabolic regulation

Introduction

Glycans, comprising polysaccharides and oligosaccharides, constitute the most abundant polymers found in nature but are far less investigated than proteins and nucleic acids (Seeberger, 2005; BeMiller, 2008). They govern a remarkably wide range of biological functions, including carbon and energy storage (Ball and Morell, 2003; Zeeman *et al*, 2010), mechanical stabilization of cells or tissues (Cosgrove, 2005), cell–cell or cell–protein interactions (Seeberger, 2005; Finkelstein, 2007) and organelle division (Yoshida *et al*, 2010). Moreover, they have attracted considerable interest as renewable energy source (Himmel *et al*, 2007; Zeeman *et al*, 2010) and starting materials or additives for many technological applications (Takaha and Smith, 1999).

Glycans can possess complex chemical structures and often occur as a polydisperse mixture of compounds with different molecular weights (BeMiller, 2008). Their biosynthesis and degradation involves the concerted action of numerous carbohydrate-active enzymes (CAZymes) (Davies and Henrissat, 2002; Coutinho *et al*, 2003; Kobayashi and Ohmae, 2006; Cantarel *et al*, 2009), which can repeatedly act on sugar donors and acceptors to generate polydispersity. Hence, two aspects complicate the description and characterization of CAZyme-mediated systems. First, polymer-active CAZymes typically do not catalyze only a single reaction and consequently rate laws with the usual kinetic (K_m and V_{max}) and thermodynamic (K_{eq}) parameters are insufficient to appropriately characterize their dynamics. Second, polydispersity implies that a huge number of variables are required to precisely describe the system. A model based on differential equations describing the temporal change of each individual species would be impractical due to potentially infinite numbers of reactants and conversions. Numerical tractability may be increased by novel rule-based approaches (Feret *et al*, 2009) or by replacing individual chemical species by a continuous mixture, leading to integro-differential equations (Aris, 1989). However, despite many experimental studies (Jones and Whelan, 1969; Lin and Preiss, 1988; Kakefuda and Duke, 1989; Colleoni *et al*, 1999; Steichen *et al*, 2008) and some attempts to model (Thoma, 1976; Nakatani, 1999) the kinetics of CAZymes, a generally applicable theoretical description is still lacking.

Our aim is to provide a general understanding of enzymes acting on polydisperse substrates. For our approach, we employ statistical thermodynamics and represent polydisperse mixtures of substrates as statistical ensembles. The thermodynamic theory allows characterizing systems with a huge number of particles by a small number of state variables, such as temperature, pressure, internal energy or entropy. We develop

an analogous description to show that the same principle holds for polydisperse reactant mixtures. In these systems, the state variable entropy has a particularly important role. If energy is neither added nor removed from the system, the equilibrium state is characterized by maximal entropy (Alberty, 2003). Conceptually, we thus follow early approaches describing chemical systems of polymers (Flory, 1944; Tobolsky, 1944). Whereas in these early studies the entropy was introduced for specific idealized conditions, we provide here a rigorous deduction from fundamental principles (Landau and Lifschitz, 1979) to arrive at a generally applicable expression of the mixing entropy (Box1; Supplementary information). A further critical advancement of our theory is the inclusion of enzymatic reactions. Enzymes catalyze changes in the polydisperse mixture. However, these changes are not completely arbitrary, but are limited to those that are in accordance with the underlying enzymatic mechanisms. Consequently, enzymatic systems acting on polydisperse mixtures are described as constrained statistical ensembles (Box 1).

To develop and experimentally validate our concept, we focus here on CAZymes catalyzing interconversions of α-1,4-glucans, intermediates in the metabolism of the most common storage polysaccharides, starch and glycogen (Ball and Morell, 2003). This class of polysaccharides consists exclusively of glucose residues linked by α-1,4 glucosidic bonds. Each distinct substrate can thus be characterized by the number of glucose residues, denoted as degree of polymerization (DP). Two CAZymes, disproportionating enzyme 2 (DPE2) and the cytosolic phosphorylase (Pho) mediate the turnover of the soluble heteroglycan (SHG) pool (Fettke *et al*, 2006, 2009b) in the cytosol of plant cells. We use this system to exemplify the utilization of polydisperse systems for metabolic regulation, thus presenting a novel interpretation for the SHG pool. This system shows how a metabolic function (carbohydrate provision and allocation) can be achieved robustly by CAZymes without requiring any additional control mechanisms such as allosteric regulations.

Results

Disproportionating enzymes increase the entropy of reaction systems

Disproportionating enzyme 1 (DPE1; Jones and Whelan, 1969; Lin and Preiss, 1988; Kakefuda and Duke, 1989; Colleoni *et al*, 1999; Critchley *et al*, 2001) is a plastidial 4-α-glucanotransferase (EC 2.4.1.25; GH77) (Takaha and Smith, 1999) catalyzing readily reversible reactions according to the equation $G_n + G_m \leftrightarrow G_{n-q} + G_{m+q}$, where G_x denotes an α-1,4-glucan with DP x, and q=1,2,3 is the number of transferred glucosyl residues (Supplementary Figure S1). All reactions occur without noticeable net enthalpy change since for every intersugar linkage cleaved another one is formed and every linkage contains approximately the same enthalpy (Goldberg *et al*, 1991), raising the question of the reaction's driving force. To the best of our knowledge, Nakatani (1999) was the first to propose, based on stochastic simulations, that in equilibrium the DP distribution has maximal entropy. Within the framework of statistical thermodynamics, it can be proven rigorously that this must indeed be the case (see Supplementary information). Moreover, our theoretical approach allows predicting the exact form of the equilibrium distribution.

In order to understand the action of enzymes like DPE1, it is helpful to interpret the distinct chemical species as different energy levels. This allows the reactant mixture to be described as a statistical ensemble (Flory, 1944; Landau and Lifschitz, 1979; Alberty, 2003). Enzymes catalyze transitions between the energy levels and the enzymatic mechanisms define which transitions are possible (Box 1; Supplementary Figure S1). Thus, enzymatic action results in a dispersal of energy. If, as is the case for DPE1, there is no net change in enthalpy, then this dispersal of energy is the only driving force of the reactions. Thus, according to the second law of thermodynamics (Landau and Lifschitz, 1979), the equilibrium distribution of the glucan mixture can be calculated by determining the maximum entropy under the constraints defined by the enzymatic mechanisms (Box 1). At equilibrium, the DPs are exponentially distributed (see Equation (3) and Box 1 Figure). The distribution is fully characterized by the exponent β (Equation 4), which depends on the average DP of the initially supplied glucans, DP_{ini}. The characteristic exponent β can be interpreted as a generalization of the equilibrium constant K_{eq} for polydisperse mixtures (Box 1).

We have experimentally tested our predictions by incubating DPE1 with defined maltodextrins. The reactions were followed until no change in the glucan patterns was detectable and the reaction system apparently reached equilibrium. The glucan patterns confirm the prediction that an exponential distribution is approximated and that the characterizing factor β depends only on the average initial DPs, DP_{ini} (Figure 1A–C; Supplementary Figure S2). Furthermore, the observed distributions quantitatively confirm the predicted decrease of β with increasing DP_{ini} (Figure 1D and E). From the observed glucan patterns, we determined the experimental entropy, which also is in accordance with the predicted entropy (Equation 5), in equilibrium (Figure 1F).

Similar to the plastidial DPE1, the cytosolic 4-α-glucanotransferase DPE2 (Chia *et al*, 2004; Fettke *et al*, 2006) mediates a randomization of α-1,4-glucans. In contrast to DPE1, DPE2 transfers single glucosyl residues only and neither utilizes maltotriose as a donor nor maltose as an acceptor (Steichen *et al*, 2008). This means that maltose molecules cannot be elongated and maltotriose molecules cannot be further shortened. Thus, whenever maltose donates a glucose residue a glucose molecule is released, and whenever glucose acts as acceptor a maltose molecule is formed. As a result, DPE2 effectively obeys an additional constraint: the conservation of the sum of glucose and maltose molecules ($x_1 + x_2$=const., see Supplementary Figure S3). Again, an exponential equilibrium distribution is predicted but the additional constraint leads to a different functional dependence of β on DP_{ini}, which is experimentally confirmed (see Supplementary Equation S57 and Supplementary Figure S4). The example of DPE2 shows the importance of recognizing constraints resulting from enzymatic mechanisms and illustrates how polydisperse mixtures relax to different equilibrium distributions when subjected to enzymes with different action patterns.

Box 1 Enzymatic reactions on polydisperse substrates

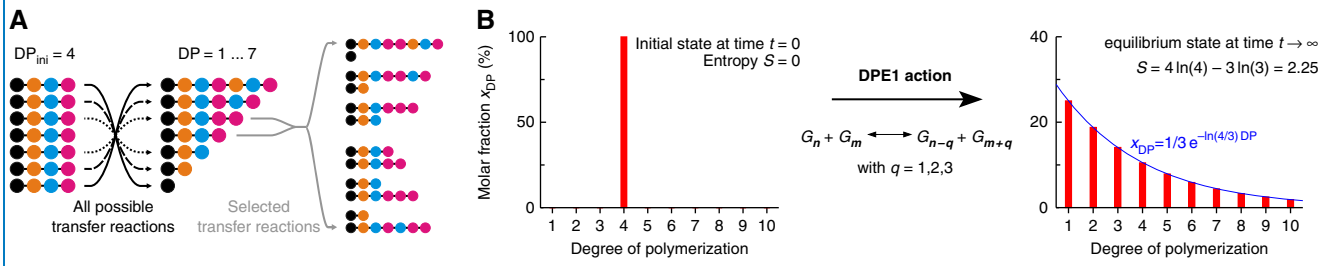

Generation of polydisperse mixtures by CAZymes: α-1,4-glucans, linear polysaccharides consisting of glucose residues that are linked by α-1,4-glucosidic bonds, are important intermediates in carbohydrate metabolism. Any such glucan can be characterized by its number of residues or degree of polymerization (DP). Glucanotransferases, such as DPE1, transfer glucosyl residues between α-1,4-glucans of any DP. Panel A illustrates the action of DPE1 for the pure initial substrate maltotetraose (DP$_{ini}$=4). All possible products of the first reaction step and a representative second step with a single pair of substrates are shown, indicating the strong diversification of the glucan pool generated by the huge number of possible reactions. Every transfer reaction conserves the number of molecules present in the reaction mixture as well as the total number of glucose residues distributed in the polydisperse pool. As a consequence, the average DP maintains the constant value DP$_{ini}$, which is in general determined by the average DP of the initially applied mixture of glucans and can assume also non-integer values. Therefore, at any time the relationships

$$\sum_{DP=1}^{\infty} x_{DP} = 1 \quad \text{and} \quad \sum_{DP=1}^{\infty} DP \cdot x_{DP} = DP_{ini} \tag{1}$$

hold, where x_{DP} describes the molar fraction of the glucan with the respective DP. This illustrates how polydisperse pools of glucans are generated by enzymatic action.

Thermodynamic description of polydisperse reactant mixtures: As any reaction, the DPE1-mediated disproportionation must proceed in the direction in which the Gibbs free energy, $G=H-TS$, decreases, where H is the enthalpy, T the temperature and S the entropy. The enthalpy H measures the energy contained in the reactants. Since the energy contained in the bonds of a glucan increases with increasing DP, the different DPs can be considered as different energy levels. The molar fractions x_{DP} can be interpreted as the occupation of the corresponding energy states. Thus, the distribution $\{x_{DP}\}$ represents a statistical ensemble which fully characterizes a polydisperse reactant mixture (Flory, 1944; Landau and Lifschitz, 1979; Alberty, 2003). The entropy S measures the dispersal of energy within the ensemble. It is defined as

$$S = -R \sum_{DP=1}^{\infty} x_{DP} \ln(x_{DP}), \tag{2}$$

where R is the universal gas constant. The DPE1-mediated transfer reactions occur without net enthalpy change, $\Delta H=0$ (Goldberg *et al*, 1991; Tewari *et al*, 1997). Consequently, decrease in Gibbs free energy is equivalent to entropy increase, which results exclusively from changes in the composition of the glucan pool. This is illustrated in panel B. At $t=0$, the reactant mixture is monodisperse and contains only maltotetraose molecules. In this case $x_4=1$ and $x_{DP}=0$ for DP $\neq 4$, resulting in $S=0$. For $t \to \infty$, the equilibrium distribution in which the energy (or interglucose bonds) is maximally dispersed is reached.

Determination of the equilibrium distribution: The equilibrium distribution can be computed by identifying those values of x_{DP}, which maximize entropy (2) under the constraints imposed by the enzymatic mechanisms. For DPE1, the constraints are given by the relationship (1) and the resulting equilibrium distribution reads

$$x_{DP} = (e^{\beta} - 1) \cdot e^{-\beta \cdot DP} \tag{3}$$

with the characteristic exponent β. For DPE1, the exponent assumes the particularly simple form

$$\beta = \ln\left(\frac{DP_{ini}}{DP_{ini} - 1}\right) \tag{4}$$

demonstrating how β fully characterizes the equilibrium in dependence on the initial substrates (see the derivation of Supplementary Equation S45 in Supplementary information). While exponential distributions as in Equation (1) are also found for the other examples considered in the text, the specific expressions for β differ due to additional constraints on the enzymatic transitions. Inserting the distribution (3) and the expression (4) for β in the expression for the entropy yields the corresponding equilibrium entropy for DPE1

$$\frac{S_{eq}}{R} = DP_{ini} \ln(DP_{ini}) - (DP_{ini} - 1) \ln(DP_{ini} - 1). \tag{5}$$

The characteristic exponent is a generalization of the equilibrium constant: The equilibrium constant K_{eq} for the single reactions can be calculated from the equilibrium concentrations (3), resulting in $K_{eq}=(x_{n-q}x_{m+q})/(x_n x_m)=1$ for every individual reaction. The functional form of β, given by Equation (4), provides additional information by revealing the dependence on the initial conditions. The exponent β is predicted to decrease when the average DP$_{ini}$ increases. Apparently, β serves as an appropriate descriptor of equilibria of polydisperse mixtures and, since it entails the equilibrium constants of the individual reactions, it can be considered as a generalization of the mass action ratio in equilibrium.

Stochastic simulations and time-resolved experiments reveal different time scales of DPE1

According to previous reports on DPE1 from white potato (Jones and Whelan, 1969), maltose is neither formed nor utilized as a glucosyl donor. These findings established the idea, that there are 'forbidden linkages' which cannot be cleaved, a rule that was later applied to DPEs from other species, such as *Arabidopsis thaliana* (Lin and Preiss, 1988)

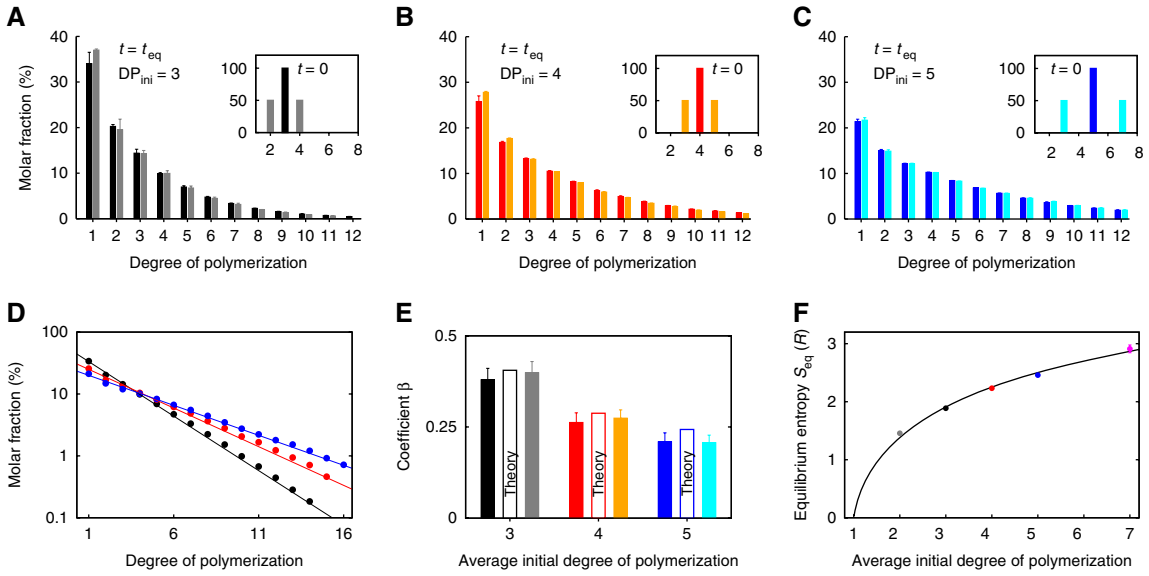

Figure 1 DPE1 maximizes entropy *in vitro*. (**A**–**C**) Experimentally determined equilibrium distributions depend only on the average degree of polymerization of the initial substrates, DP_{ini}. All DP patterns obey the theoretically expected exponential distribution where the exponential factor β depends on the initial substrates, as demonstrated by maltotriose G_3 (black in A), maltotetraose G_4 (red in B) and maltopentaose G_5 (blue in C). The distributions are independent of how DP_{ini} is realized. In each panel, the distributions obtained from two different initial conditions with identical DP_{ini} are indistinguishable (G_3 and a 1:1 mixture of G_2 and G_4 (gray) in (A), G_4 and a 1:1 mixture of G_3 and G_5 (orange) in (B), G_5 and a 1:1 mixture of G_3 and G_7 (cyan) in (C)). (**D**) Comparison between the experimental results (dots) and the theoretical predictions (solid lines) in a semi-log plot demonstrates the differences of the coefficients β (corresponding to the slopes) for different initial substrates. (**E**) Agreement of observed and predicted β demonstrates the entropic mechanism of glucanotransferases. (**F**) The experimentally determined equilibrium entropies S_{eq} (dots) in dependence on the average initial degree of polymerization (DP_{ini}) match with the values predicted by Equation (5), indicated by the solid line. Distributions for DP_{ini}=2 and DP_{ini}=7 are shown in Supplementary Figures S2B and S5B, respectively. (All error bars denote standard deviation of three independent experiments.) Source data is available for this figure in the Supplementary information.

and *Chlamydomonas reinhardtii* (Colleoni *et al*, 1999). However, our measurements (Figure 2) clearly demonstrate that this rule is not valid at least for recombinant DPE1 from *A. thaliana*. Presumably, this discrepancy is due to differences in the length of the incubation period. As revealed by our measurements, ∼10 min after incubation a quasi-stationary equilibrium is reached in which maltose is undetectable. Subsequently, maltose levels rise and approach the theoretically predicted equilibrium with a much lower rate after several days (Figure 2A). These data are consistent with the assumption that 4-α-glucanotransferases prefer distinct glucan binding modes (Suganuma *et al*, 1991; Nakatani, 1999, 2002; Takaha and Smith, 1999). Based on this view, we developed a stochastic model which reproduces the observed time-resolved glucan patterns under the sole assumption that glucosyl transfers occur with an 800-fold smaller probability than transfers of maltosyl or maltotriosyl residues (Figure 2A). The two time scales can be identified by following the change in mixing entropy (Figure 2B). The quasi equilibrium entropy (dotted line in Figure 2B) is theoretically calculated by excluding maltose from the ensemble representing the polydisperse mixture (see Supplementary Equation S48 in Supplementary information). In the vicinity of the quasi equilibrium, the mixing entropy increases more slowly, while steadily evolving toward the predicted maximum entropy state. Our simulations demonstrate that three kinetic constants are sufficient to characterize the DPE1-mediated system: one rate constant reflecting maximal turnover and two constants describing different transfer probabilities reflecting different subsite affinities at the substrate binding domain (Thoma *et al*, 1971; Suganuma *et al*, 1991; Nakatani, 1999). Experimentally, these values are not accessible through simple incubation experiments in analogy to the classical treatment of enzymes catalyzing single reactions, but rather require monitoring of the entire reactant mixture. An alternative description based on two maximal turnover constants can reproduce the same kinetics but is biochemically less plausible. Glycoside hydrolase domains usually possess several binding subsites which allow for different alignments of the substrate formed with different probabilities (Thoma *et al*, 1971). In contrast, the transfer step always acts between well-defined subsites irrespective of the actual alignment of the substrate (Barends *et al*, 2007).

Generalization for energetically open systems

The interpretation of the distinct reactants as different energy states offers a straightforward generalization to reaction systems in which bond enthalpy is not conserved. Taking into account the sum of energies of formation g^f, the equilibrium is determined by a minimum in Gibbs free energy (Alberty, 2003) given by $g=g^f-TS$, where T is the temperature and S the entropy (cf. Supplementary Equation S31 in Supplementary information).

First, we consider the reaction system catalyzed by α-glucan phosphorylase (Pho; EC 2.4.1.1; GT35). Reversibly transferring terminal glucosyl residues from the non-reducing ends of soluble glucans to orthophosphate, this CAZyme does not conserve the

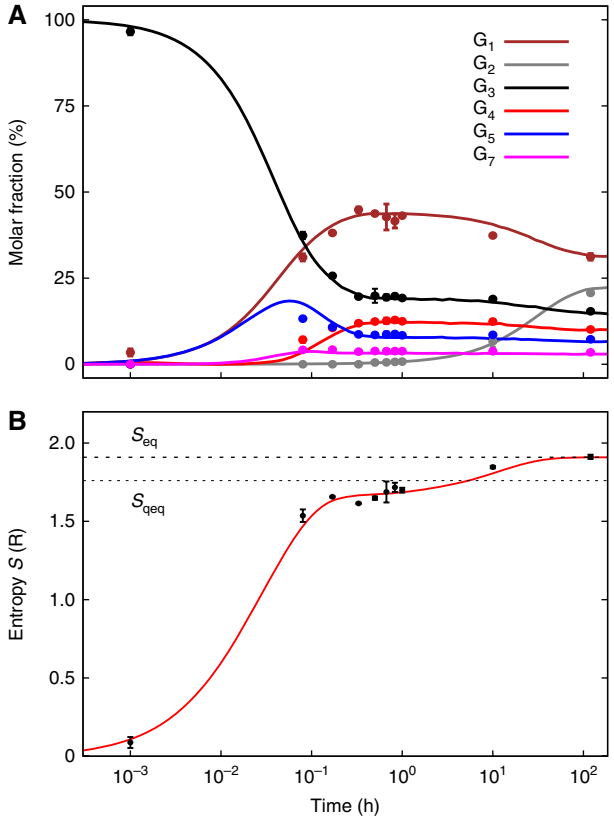

Figure 2 Low binding affinity for maltose induces a quasi equilibrium distribution. (**A**) The experimental time course (dots) shows the generation of the different glucans for DPE1 incubated with maltotriose, demonstrating that maltose is produced on a slower time scale compared with the other glucans. Stochastic simulations (solid lines) assuming an 800-fold reduced probability for the transfer of single glucosyl residues compared with maltosyl and maltotriosyl residues accurately reproduce the data. (**B**) The increase in entropy exhibits two time scales. In the first phase, the entropy rapidly increases toward a quasi equilibrium state without detectable maltose. The dotted line at S_{qeq} indicates the predicted equilibrium entropy for a constrained system not capable of producing maltose (see Supplementary information). The second phase is characterized by a much slower relaxation towards the real equilibrium S_{eq} (dashed line). The corresponding temporal DP distributions are shown in Supplementary Movie. (All error bars describe standard deviation of three independent experiments.). Source data is available for this figure in the Supplementary information.

bond enthalpy since it replaces a glucosidic by an ester bond. The resulting equilibrium distribution for different initial conditions, predicted by minimizing the Gibbs free energy, is described by an implicit equation, $f(\beta, \mathrm{DP_{ini}}, T; \Delta g) = 0$, which additionally depends on the difference in the enthalpies of bond formation, Δg (see Supplementary Equation S68 in Supplementary information). The predictions are experimentally confirmed by *in vitro* experiments (Figure 3).

Exothermic reactions shift equilibrium distributions

As a prototype of a multi-enzyme system, we consider the action of DPE1 in the presence of hexokinase (HK, EC 2.7.1.1), which phosphorylates glucose at the expense of ATP to produce glucose-6-phosphate and ADP. In this direction, the reaction is exothermic and its equilibrium is experimentally controlled by the ATP level. Since the HK reaction diminishes the glucose pool accessible to DPE1 but keeps the number of interglucose bonds constant, the equilibrium pattern of the glucans is shifted toward larger DPs (Figure 4; Supplementary Figure S5). This result concurs with earlier findings (Walker and Whelan, 1959; Kakefuda and Duke, 1989) showing the capability of DPE1 to synthesize amylose, which now experience a quantitative theoretical explanation. The predicted exponential distribution of the equilibrium pattern is again accurately described by the parameter β. Here,

$$g^{\mathrm{f}} = u \cdot \Delta g \quad \text{and}$$

$$S = -R\left(u\ln(u) + a_2\ln(a_2) + a_3\ln(a_3) + \sum_{\mathrm{DP}=1}^{\infty} x_{\mathrm{DP}}\ln(x_{\mathrm{DP}})\right),$$

where u is the molar fraction of glucose-6-phosphate, a_2 and a_3 are the molar fractions of ADP and ATP, respectively, and Δg is the molar Gibbs energy of the HK reaction. Minimizing the Gibbs energy results in an implicit equation for $\beta = \beta(\mathrm{DP_{ini}}, \mathrm{ATP}, T; \Delta g)$, which now additionally depends on the applied ATP level and the equilibrium constant of HK (see Figure 4B and Supplementary Equation S84 in Supplementary information).

Physiological significance of entropy and polydisperse systems

The proposed description of CAZymes provides a novel way to characterize enzymes acting on polydisperse substrates, resolving some of the discrepancies in previous studies on DPEs. Because mixing entropy has a pivotal role in these systems we call the associated enzymes entropic. This is not to be confused with the supposed entropic effect on enzymatic rates associated with reducing the molecular degrees of freedom upon substrate binding (Jencks, 1997; Warshel *et al*, 2006). In the following, we discuss how randomization of the metabolite pool and the associated entropy increase are used constructively for establishing important physiological functions.

The thermodynamic analysis sheds new light on several aspects of glycan metabolism in plants (Critchley *et al*, 2001; Stitt *et al*, 2010; Zeeman *et al*, 2010). When the plastidial HK or the glucose exporter is active, glucose molecules are removed from the polydisperse pool of α-1,4-glucans and are therefore no longer available as acceptor substrates for the DPE1-mediated transfer reactions. Our results (Figure 4) suggest that under these conditions DPE1 mediates an energy-independent elongation of glucans and thereby provides substrates for the plastidic α-glucan phosphorylase or even supports starch synthesis directly. The latter conjecture is consistent with the phenotype of a *C. reinhardtii* mutant lacking a functional DPE1 which displays aberrant starch synthesis (Colleoni *et al*, 1999).

Entropy-induced robustness

Stochastic simulations allow us to investigate the role of enzymes generating mixing entropy in non-equilibrium open systems. Here, we want to exemplify this for carbon metabolism in plants.

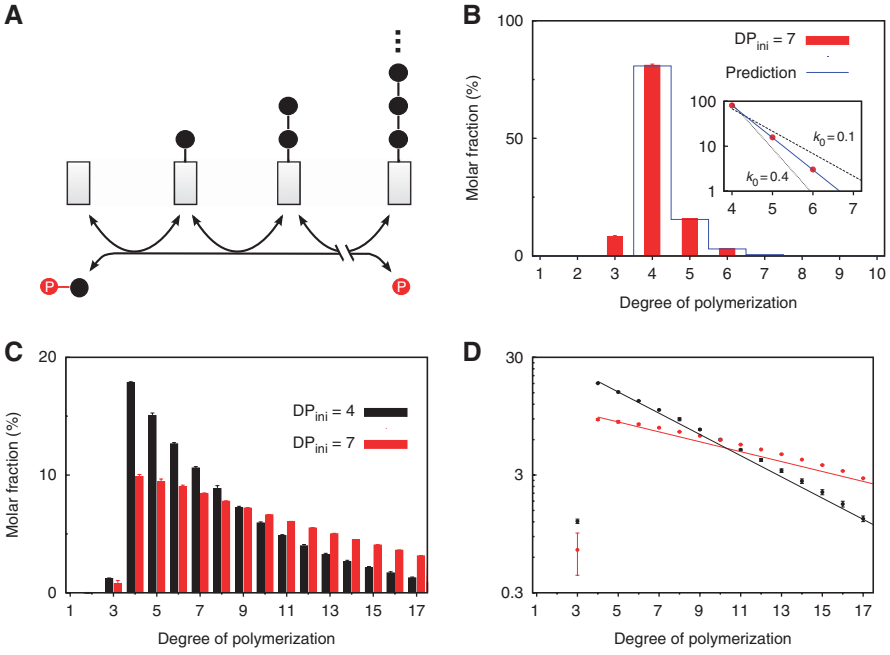

Figure 3 Equilibrium distributions of the degree of polymerization for phosphorylase experiments. (**A**) Schematic representation of the mechanism of phosphorylase. From an α-1,4-linked glucan chain, one glucose residue is reversibly transferred to orthophosphate (red), producing glucose-1-phosphate (G1P). The gray box represents any primer molecule, which can also be a glucan. (**B**) The experimental distribution (red bars) for a 1:50 mixture of DP_{ini}=7 and orthophosphate exhibits a steep decrease. From the theoretical prediction (See Supplementary Equation S68) shown in blue, we can fit the unknown parameter $k_0 = \exp(-\Delta g/RT)$ as 0.19. The inlet shows the logarithmic data (red) and further predictions for k_0=0.1 (dashed) and k_0=0.4 (solid). (**C**) Comparison between G_4 (black) and G_7 (red) incubated with G1P in a 1:4 ratio demonstrates the dependence on the initial substrate. (**D**) Both distributions obey an exponential distribution as shown by the logarithmic plot. The agreement of experiments (dots) and theoretical predictions (lines) validates the theoretical approach. (Error bars indicate standard deviation of three independent experiments.). Source data is available for this figure in the Supplementary information.

A key process in plants is the starch-to-sucrose pathway in leaf cells during darkness (Smith *et al*, 2005; Fettke *et al*, 2009a). Transitory starch degradation in chloroplasts essentially provides maltose, which is exported to the cytosol in order to support glycolysis as well as sucrose synthesis. Glycolysis is the ubiquitous pathway of energy metabolism to produce chemical energy equivalents in form of ATP, and sucrose is the major form in which carbon is transported to sink organs of plants. It turns out that by exporting maltose, using it as a glucosyl donor (DPE2), plants can bypass the first ATP-dependent reaction of glycolysis (hexokinase) and produce the intermediate glucose-1-phosphate (G1P) via phosphorolysis (α-glucan phosphorylase) of a soluble pool of heteroglycans (SHG; Lu and Sharkey, 2004; Fettke *et al*, 2009b). G1P serves as a substrate for both the downstream processes of glycolysis and sucrose synthesis.

Notably, Arabidopsis leaf cells contain around 100 chloroplasts, and starch content and degradation rate may vary considerably depending on external conditions such as light intensity or day length (Gibon *et al*, 2004; Graf and Smith, 2011). Maltose export occurs locally through the specific maltose exporter MEX1 (Niittylä *et al*, 2004) leading to inhomogeneous maltose concentrations in the cytosol. A challenge for the plant is to integrate fluctuating carbon fluxes in a way that ensures stable levels of substrates for downstream processes, in particular glucose and G1P. Moreover, the supply of these substrates has to be temporarily ensured during light-dark transitions. It has been hypothesized that these buffering functions are provided by the SHG pool (Fettke *et al*, 2009a), but no conclusive mechanistic explanation exists how these functions are achieved. Interestingly, a significant mass fraction of the SHG pool consists of glucose residues, which are added and removed by DPE2 and cytosolic α-glucan phosphorylase (Pho), two 'entropic enzymes' characterized in this work. Thus, it is tempting to suggest that the entropy-driven maintenance of polydispersity by these enzymes provides an explanation for the role of SHG in buffering carbon fluxes.

A minimal model which mimics the physiological scenario found in the cytosol of plant leaves during darkness is shown in Figure 5A. In order to study the role of the SHG pool, we compare this system with an alternative one in which mixing entropy does not play a role. We consider a noisy maltose input, which may for example result from an inhomogeneous transport of maltose (G2) into the cytosol. A single process consuming G1P and glucose (G1) represents the activity of downstream pathways. We study the output performance for two mechanisms: (1) maltose is converted into glucose and G1P by the concerted action of the entropic enzymes DPE2 and Pho; (2) maltose is directly split by a single reaction according to $G2 + Pi \leftrightarrow G1 + G1P$, which could for example be catalyzed by maltose phosphorylase (MPho, EC 2.4.1.8). While system 2 depends on a classical enzyme catalyzing one specific reaction, the enzymes of system 1 produce a polydisperse pool of metabolites. As demonstrated above, an important contribution of the driving force of these enzymes is an increase in the mixing entropy of the reactant mixture (see also Sections S2.2 and S2.3 in Supplementary information). In this

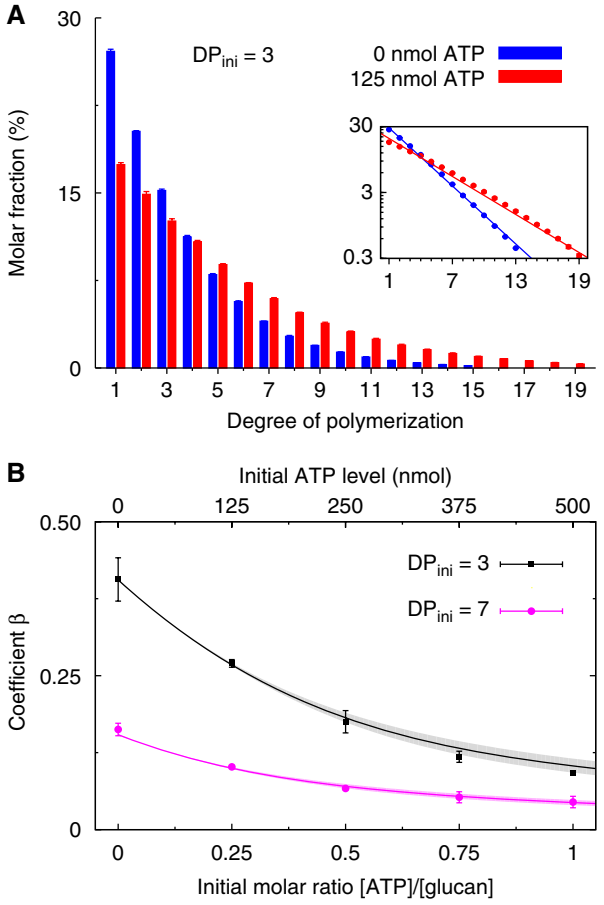

Figure 4 Energetically unbalanced reactions affect the equilibrium parameter β. In the presence of hexokinase (HK), the DPE1-mediated equilibrium distribution depends on the applied amount of ATP, the Gibbs energy of the HK reaction and the average initial degree of polymerization, DP_{ini}. (**A**) The equilibrium distribution of DPE1 incubated with 500 nmol maltotriose (G_3) and 125 nmol ATP (red) is shifted toward longer DPs compared with the distribution without ATP (blue). The semi-logarithmic plot (inset) shows that observed (circles) and predicted (lines) distributions are in good agreement. (**B**) In systematic experiments, the ATP level was varied between 0 and 500 nmol leading to an ATP/glucan ratio between 0 and 1 for the two different initial substrates G_3 (black) and G_7 (magenta). From distributions corresponding to those in (A), the equilibrium parameter β was determined by fitting to data (symbols) and compared with the theoretical prediction (lines) according to Supplementary Equation S84 (see Supplementary information). Predictions were calculated with the experimentally determined average equilibrium constant of the HK reaction. Shadowed regions describe the corresponding standard deviation of four independent experiments. (All error bars correspond to standard deviation of three independent experiments.). Source data is available for this figure in the Supplementary information.

sense, system 1 is, in contrast to system 2, to a large extent driven by entropy gradients, defined as the change of entropy with reaction progress (Wicken, 1978).

The downstream activity represented by the G1P output rate differs for the two systems. As shown in Figure 5B, the MPho system (red) strongly follows the noisy input leading to large fluctuations in downstream activity, whereas the increased internal entropy due to the SHG buffer (blue) dampens the fast fluctuations. Although the MPho system can reach higher output rates, the SHG system exhibits a larger physiological robustness because in case of starvation it can, for a limited time, still provide energy from buffered glucans with larger DPs. This is visible by the exponential damping of metabolic activity after setting the influx to very small values at around 8000 s in Figure 5B.

Analyzing the dependence of the output on the maltose influx into the (cytoslic) system (Figure 5C) demonstrates that the SHG system exhibits a rather constant metabolic activity independent of the influx strength as long as the temporal average of the input does not vary too much. In contrast, the MPho system reacts nearly immediately to changes in the input as shown by the linear relation. To summarize, this system exemplifies how cells may exploit mixing entropy in metabolism to (a) attenuate rapid fluctuations, thus functioning like a low-pass filter, (b) allow for transient support of downstream activity after a drop in maltose influx through buffering and (c) integrate largely varying influxes to achieve a constant output activity in a robust manner.

For two reasons, a simple buffering by high maltose levels is biologically not feasible (Sharkey *et al*, 2004): first, high maltose levels are toxic to the plant and second, it would imply a high osmotic pressure on leaf cells because the plasma membrane is impermeable for maltose.

A low-pass filter could in principle also be achieved by a monodisperse maltose buffer, in which maltose is bound to a hypothetical buffer molecule with a higher capture rate compared with its release rate (see Section S3.2 in Supplementary information and Supplementary Figure S6). However, this would again lead to a high osmotic pressure since the buffer concentration has to be large in order to compensate fluctuations. Furthermore, cells would need to regulate the buffer concentration in dependence on the ratio of maltose influx to glycolytic activity. In case of high maltose influx, the buffer becomes saturated, leading to a reduced capability to dampen fluctuations. This can only be compensated by further buffer production. The SHG buffer mechanism circumvents these problems. First, high osmotic pressure is avoided because of its polydispersity. Second, the buffer size is intrinsically regulated because accumulation of maltose will simply lead to the production of glucans with a longer DP without the need to increase the concentration of buffering molecules.

Discussion

Although the description of polydisperse mixtures in the framework of statistical thermodynamics is well established in chemistry (Flory, 1944; Tobolsky, 1944), its appropriate adaptation to biochemical reaction systems is still lacking. We have here provided a rigorous derivation to describe polydisperse reaction mixtures and have shown that enzymes can be incorporated into this thermodynamic picture by constraints imposed by their molecular mechanisms. By establishing the bridge between biochemistry and physics, we provide a novel way to describe, predict and understand the behavior of the important class of biological systems involving enzymatic reactions on polymers. Specifically, the action patterns of CAZymes can be understood by introducing the mixing entropy of the polydisperse glycan pool as an important state variable. Applying the principle of constrained entropy maximization to systems of 'entropic' enzymes allows for

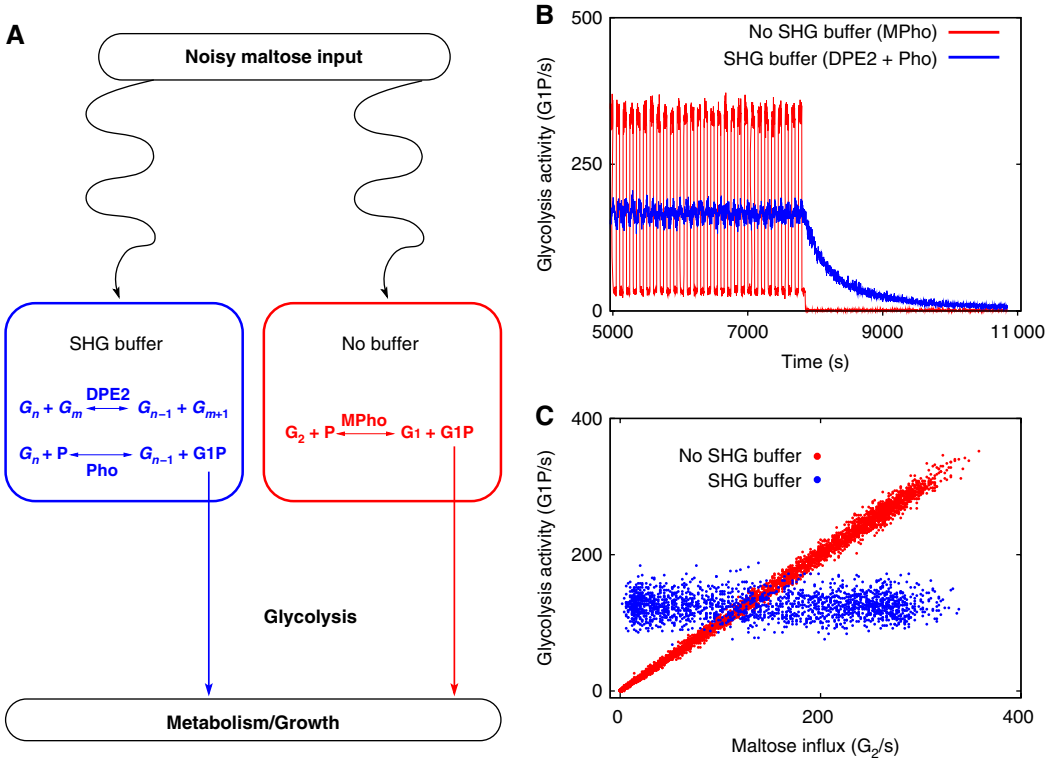

Figure 5 Entropic enzymes induce metabolic robustness. (**A**) We compare the downstream activity of a system with the entropic enzymes DPE2 (blue) and Pho (magenta) catalyzing the turnover of an SHG pool with a system which directly converts a fluctuating maltose input into glucose (G_1) and glucose-1-phosphate (G1P) using maltose phosphorylase (MPho, red). (**B**) The simulated temporally resolved output activity indicates that the higher entropy due to the SHG pool smears out the large fluctuation of the noisy maltose influx while the MPho system follows the fluctuations rapidly. The difference becomes dramatic in the case of very small maltose influx, where the downstream activity of the MPho system stops abruptly whereas the SHG buffer system can still provide energy from the pool of larger glucans. (**C**) The dependence of the G1P output on the maltose input demonstrates that the SHG pool acts as a buffer and ensures a robust support of downstream metabolism with carbon even under large and rapid external fluctuations, whereas the MPho system reacts strongly to changes in influx.

correct predictions of equilibrium distributions, which has not been easily possible with previous approaches, and sheds new light on regulatory mechanisms.

Knowledge of the equilibrium is useful to determine in which direction a system will evolve. However, to describe living systems, which operate far from equilibrium, information about the kinetics is necessary. To explore the dynamics of glycan metabolism, we have conducted stochastic simulations. Exemplified by DPE1, we demonstrated how comparing time-resolved *in vitro* data with simulated trajectories could elucidate molecular mechanisms of CAZymes. Computational studies of the SHG pool, which is maintained and turned over by two entropic enzymes, provided a novel explanation of its biological function. The latter example is illustrative of how mixing entropy is effectively used to establish a robust buffering and integrating function. We expect that this example may serve as a prototype for future interpretations of structurally similar entropy-driven metabolic systems.

Apparent analogies are, for example, found in the carbohydrate metabolism of yeast. Glycogen chains are elongated by the glycogen synthase (Gsy1p/Gsy2p) when yeast is growing on a fermentable carbon source (Francois and Parrou, 2001). Glycogen degradation involves the two entropic enzymes glycogen phosphorylase (Gph1p), which releases G1P from glycogen much alike the phosphorylase Pho studied here, and the debranching enzyme (Gdb1p), which transfers maltosyl residues between glycogen chains in analogy to the disproportionating enzymes and releases glucose from branch points. These striking similarities allow us to conjecture that the concerted enzyme actions generate a polydisperse buffer that functions according to the same principles as the SHG buffer in plants. During diauxic shift, when fermentable carbon sources are depleted, the turnover of this buffer will have an important role for the temporary provision of glucose for downstream processes (Lillie and Pringle, 1980). Considering that resulting changes in gene expression profiles (Chu *et al*, 1998) depend on cellular glucose metabolism, our approach forms the basis for a quantitative and mechanistic description of the connections between metabolic and genetic responses to varying environmental conditions. This enables new insights into the fundamental question as to how environmental factors such as limitation of nutrients (Parrou *et al*, 1999) determine the dynamic phenotypic responses for a given genotype.

Supported by our empirical evidence for CAZymes, we expect that the entropic viewpoint on biochemical reactions in general (Wicken, 1978) and the principle of constrained entropy maximization in particular (Landau and Lifschitz, 1979; Craig, 1992) provide a sound framework applicable to metabolic reaction networks beyond the examples presented herein. Our concept offers a shift in perspective by suggesting

that cellular metabolism is organized as an intricate interplay of energy- and entropy-driven processes. Apparently, living cells have evolved to use internal entropy gradients constructively to increase efficiency and robustness.

Materials and methods

Chemicals

ATP was purchased from Roche (product no. 10519979001, Mannheim, Germany). Maltose (product no. EC 200-716-5), α-glucans, glucose 1-phosphate (product no. EC 260-154-1) and glycogen (from oyster, type II) were obtained from Sigma-Aldrich (Taufkirchen, Germany). Recombinant plastidial α-glucan phosphorylase (Pho1) from *Oryza sativa* was expressed and purified as described elsewhere (Fettke *et al*, 2010).

Cloning procedure

For cloning of dpe1 (At5g64860) and dpe2 (At2g40840) from *Arabidopsis thaliana*, total RNA was isolated from leaves (100 mg fresh weight each) by using the Nucleo Spin RNA Plant Kit (Machery-Nagel, Düren, Germany).

For first-strand cDNA synthesis encoding DPE1, the SuperScript II Reverse Transcriptase (Invitrogen, Darmstadt, Germany) and a specific 3′ primer (5′–3′) AAGCCGTCCGTACAATGACAAAAGATCTCT were used following the instructions of the manufacturer. The resulting cDNA was then amplified by PCR using the *Eco*RI and *Xho*I linked primers (5′ forward primer (5′–3′) GAATCCGATGGAGGTCGTT TCGAGTAATTC and 3′ reverse primer (5′–3′) CTCGAGAAGCCGTCCG TACAATGAACCAAG) that include the complete cDNA except the predicted transit sequence (135 bp from the start). In a final volume of 50 μl, the PCR mixture contained 2 μl of the reverse transcription mixture and Phusion Taq Polymerase (Finnzymes, Espoo, Finland). Subsequently, the 2.2-kb dpe1 encoding fragment was subcloned into pGEM-T easy vector (Promega, Mannheim, Germany). Finally, the dpe1 fragment was restricted by *Eco*RI/*Xho*I and ligated to the expression vector pET23b (Novagen, Darmstadt, Germany).

For cloning of dpe2, first-strand cDNA was synthesized by using the 3′ primer (5′–3′) TTATGGGTTTGGCTTAGTCGAGCCATTGGC (see above) and was then amplified by HF Polymerase (product no. 11732650001, Roche) by use of the following primers: 5′ forward primer (5′–3′) ATGATGAATCTAGGATCTCTTTCGTTGAG and 3′ reverse primer (5′–3′) TTATGGGTTTGGCTTAGTCGAGCCATTGGC. Subsequently, the dpe2 encoding cDNA was ligated to the pGEM-T easy vector. Subcloning was performed by the Gateway Technology (Invitrogen) following the instructions of the manufacturer. Subsequently, the pDONR221 was recombined with the attB1- and attB2-flanked dpe2 cDNA (primers: attB1 (5′–3′) AAAAAGCAGGCTTAATGATGAATCTAG GAT and attB2 (5′–3′) AGAAAGCTGGGTATGGGTTTGGCTTAGTCG). Finally, the PCR product was cloned into pDEST17.

DPE1 and DPE2 were expressed in *E. coli* BL21 (DE3) harboring the plasmid pET23b and pDEST17, respectively. Cells were grown in LB medium containing 100 μg ml^{-1} ampicillin at 37°C until the suspension reached an OD_{600} of ∼0.8. Following the addition of IPTG (final concentration 1 mM), the suspension was cooled to 18°C and incubated overnight. Cells were harvested, washed with 50 mM Tris–HCl (pH 7.5), resuspended in grinding buffer (20 mM NaH_2PO_4, 500 mM NaCl, 2.5 mM DTT, 20 mM imidazole and 1% [v/v] protease inhibitor cocktail III (Calbiochem, Darmstadt, Germany), pH 7.4) and sonicated on ice. Following centrifugation (20 min at 20 000 *g*), the supernatant was passed through a nitrocellulose filter (pore size 0.45 μm) and the filtrate was loaded onto a HisTrap-HP column (1 ml; GE Healthcare, München, Germany). For elution, a stepwise increasing imidazole concentration (up to 500 mM, dissolved in grinding buffer) was used. Fractions containing the desired protein were combined, concentrated and were then transferred to storage buffer (50 mM Hepes-KOH, pH 7.5, 1 mM EDTA, 2 mM DTT), using Amicon Ultra-4 centrifugal filter-unit concentrator (MWCO 30 000, Millipore, Schwalbach am Taunus, Germany). Finally, glycerol was added (final concentration of 20% [v/v]) and aliquots were frozen at −80°C.

Capillary electrophoresis

Glucans were separated from denatured proteins by using a centrifugal filter device (YM-30; Microcon, Millipore) and were freeze dried. Each sample was diluted in 2 μl 0.2 M 8-aminopyrene-1,3,6-trisulfonic acid (APTS) in 15% [v/v] aqueous acetic acid plus 2 μl 1 M Na-cyanoborohydride. Following incubation (4 h at 37°C) and 250–500-fold dilution with water, the labeled samples were applied to capillary electrophoresis (CE) using a PA-800 (Beckman Coulter, Krefeld, Germany).

Protein concentrations

Soluble proteins were quantified using Bio-Rad protein assay (Bio-Rad, München, Germany). BSA served as standard (Roth, Karlsruhe, Germany).

Photometric assay of the activity of recombinant DPE1 and DPE2 (PA)

Activity was measured using a slightly modified version of the coupled photometric assay described by Lu *et al* (2006). For DPE1, maltotriose (final concentration 2 mM) served as substrate. The assay of DPE2 contained maltose (2 mM maltose) and glycogen from oyster (1 mg ml^{-1}; final concentrations each).

Long-term assay of the recombinant transferases (LTA)

For LTA, all reaction mixtures containing 0.025% [w/v] sodium azide were incubated at 30°C for several days. The following reaction mixtures were used: (a) DPE1 or DPE2 (25 mU each; 100 μl final volume) was incubated with 500 nmol α-glucans, 2.5 mM citrate-NaOH (pH 7.0). In some experiments, the citrate buffer was replaced by 25 mM Hepes-KOH (pH 7.0). Under these conditions, the same α-glucan patterns were observed. (b) DPE1/ATP: DPE1 (25 mU DPE1 each; 100 μl final volume), 25 mM Hepes-KOH (pH 7.0), 6.5 mM $MgCl_2$, 500 nmol maltotriose or maltoheptaose, 0–500 nmol ATP and 500 mU hexokinase (from yeast, Roche). (c) Pho1/G1P: Pho1 (0.5 μg each; 100 μl final volume), 25 mM Hepes-KOH (pH 7.0), 1 μmol G1P, 250 nmol maltotetraose or 250 nmol maltoheptaose. (d) Pho1/Pi: Pho1 (0.5 μg; 100 μl final volume), 25 mM Hepes-KOH (pH 7.0), 250 nmol maltoheptaose, 12.5 μmol orthophosphate.

All enzymes were replaced by a fresh preparation every day. At intervals, aliquots (equivalent to 50 nmol α-glucans) were withdrawn and reactions were terminated by heating (95°C for 5 min). Patterns of α-glucans were monitored by CE following coupling to APTS.

Simulations

We simulate the reaction systems by a Gillespie algorithm (Gillespie, 1977) where we consider the binding of the donor and the acceptor to the enzyme explicitly. Thus, in each reaction step one of the following reaction is performed $E + G_n \rightarrow EG_n$ and $EG_n + G_m \rightarrow G_{n-q} + G_{m+q} + E$, where E denotes the free enzyme and G_n the donor with DP=n, G_m is the acceptor with DP=m and EG_n describes the enzyme–donor complex. The reaction occurs in dependence on the propensities defined by the number of molecules times the reaction rate constants. In case of DPE1, the binding reaction rate for the donor k_d depends on the binding mode, that is, on the number q of glucosyl residues to be transferred. The time-resolved experiments were simulated with $k_d(q=1)=0.00025\ s^{-1}$ and $k_d(q=2,3)=0.2\ s^{-1}$ and the constant acceptor binding rate $k_a=0.2\ s^{-1}$. For DPE2, k_d is non-zero for $q=1$ only and equals $k_a=0.1\ s^{-1}$. The phosphorylase was simulated according to the reversible reaction given by Supplementary Equation S58 where the phosphorylation occurs with rate $k_p=0.1\ s^{-1}$ and dephosphorylation with rate $k_{dp}=k_p/\exp(-\Delta g/RT)$, where the difference in bond enthalpy Δg was fitted from experiments with an extreme 50:1 ratio of Pi:G_7 (see Figure 3). For further details on the simulations, see Text S3 in Supplementary information.

Supplementary information

Supplementary information is available at the *Molecular Systems Biology* website (www.nature.com/msb).

Acknowledgements

We express our sincerest thanks to Martin Steup for his continuous support and provision of lab space and reagents. We thank J Garcia-Ojalvo, M Kschischo, K Chandrasekaran and H-G Holzhütter for critically reading the manuscript, their helpful comments and encouraging remarks. This work was financially supported by the German Federal Ministry of Education and Research (*Go*FORSYS initiative, ÖK and OE; FORSYS-Partners initiative, ÖK and AS), the Scottish Universities Life Science Alliance, SULSA, and the European Union (TiMet, OE).

Author contributions: OE and ÖK initiated and conceptually outlined the work. The analytic calculations were performed by ÖK and OE, and AS was involved in the further development of the theory and conducted the stochastic simulations. The experiments were designed by SM in discussion with all authors. SM performed the experiments. All authors contributed to data analysis and to the preparation of the manuscript.

Conflict of interest

The authors declare that they have no conflict of interest.

References

Alberty RA (2003) *Thermodynamics of Biochemical Reactions*. Hoboken, USA: John Wiley & Sons

Aris R (1989) Reactions in continuous mixtures. *AIChE J* **35:** 539–548

Ball SG, Morell MK (2003) From bacterial glycogen to starch: understanding the biogenesis of the plant starch granule. *Annu Rev Plant Biol* **54:** 207–233

Barends TRM, Bultema JB, Kaper T, van der Maarel MJEC, Dijkhuizen L, Dijkstra BW (2007) Three-way stabilization of the covalent intermediate in amylomaltase, an α-amylase-like transglycosylase. *J Biol Chem* **282:** 17242–17249

BeMiller JN (2008) *Polysaccharides: Occurrence, Significance, and Properties*. Fraser-Reid BO, Tatsuta K and Thiem J (eds) pp. 1413–1435. Berlin/Heidelberg: Springer Verlag

Cantarel BL, Coutinho PM, Rancurel C, Bernard T, Lombard V, Henrissat B (2009) The Carbohydrate-Active EnZymes database (CAZy): an expert resource for glycogenomics. *Nucleic Acids Res* **37:** D233–D238

Chia T, Thorneycroft D, Chapple A, Messerli G, Chen J, Zeeman SC, Smith SM, Smith AM (2004) A cytosolic glucosyltransferase is required for conversion of starch to sucrose in Arabidopsis leaves at night. *Plant J* **37:** 853–863

Colleoni C, Dauvillée D, Mouille G, Morell M, Samuel M, Slomiany MC, Liénard L, Wattebled F, d'Hulst C, Ball S (1999) Biochemical characterization of the *Chlamydomonas reinhardtii* α-1,4 glucanotransferase supports a direct function in amylopectin biosynthesis. *Plant Physiol* **120:** 1005–1014

Cosgrove DJ (2005) Growth of the plant cell wall. *Nat Rev Mol Cell Biol* **6:** 850–861

Coutinho PM, Deleury E, Davies GJ, Henrissat B (2003) An evolving hierarchical family classification for glycosyltransferases. *J Mol Biol* **328:** 307–317

Craig NC (1992) *Entropy Analysis: An Introduction to Chemical Thermodynamics*. New York, USA: VCH Publishers

Critchley JH, Zeeman SC, Takaha T, Smith AM, Smith SM (2001) A critical role for disproportionating enzyme in starch breakdown is revealed by a knock-out mutation in Arabidopsis. *Plant J* **26:** 89–100

Chu S, DeRisi J, Eisen M, Mulholland J, Botstein D, Brown PO, Herskowitz I (1998) The transcriptional program of sporulation in budding yeast. *Science* **282:** 699–705

Davies GJ, Henrissat B (2002) Structural enzymology of carbohydrate-active enzymes: implications for the post-genomic era. *Biochem Soc Trans* **30:** 291–297

Feret J, Danos V, Krivine J, Harmer R, Fontana W (2009) Internal coarse-graining of molecular systems. *Proc Natl Acad Sci USA* **106:** 6453–6458

Fettke J, Chia T, Eckermann N, Smith AM, Steup M (2006) A transglucosidase necessary for starch degradation and maltose metabolism in leaves at night acts on cytosolic heteroglycans (SHG). *Plant J* **46:** 668–684

Fettke J, Hejazi M, Smirnova J, Höchel E, Stage M, Steup M (2009a) Eukaryotic starch degradation: integration of plastidial and cytosolic pathways. *J Exp Bot* **60:** 2907–2922

Fettke J, Malinova I, Albrecht T, Hejazi M, Steup M (2010) Glucose-1-phosphate transport into protoplasts and chloroplasts from leaves of Arabidopsis. *Plant Physiol* **155:** 1723–1734

Fettke J, Malinova I, Eckermann N, Steup M (2009b) Cytosolic heteroglycans in photoautotrophic and heterotrophic plant cells. *Phytochemistry* **70:** 696–702

Finkelstein J (2007) Glycochemistry and glycobiology. *Nature* **446:** 999

Flory PJ (1944) Thermodynamics of heterogeneous polymers and their solutions. *J Chem Phys* **12:** 425–438

Francois J, Parrou JL (2001) Reserve carbohydrates metabolism in the yeast *Saccharomyces cerevisiae*. *FEMS Microbiol Rev* **25:** 125–145

Gibon Y, Bläsing OE, Palacios-Rojas N, Pankovic D, Hendriks JHM, Fisahn J, Höhne M, Günther M, Stitt M (2004) Adjustment of diurnal starch turnover to short days: depletion of sugar during the night leads to a temporary inhibition of carbohydrate utilization, accumulation of sugars and post-translational activation of ADP-glucose pyrophosphorylase in the following light period. *Plant J* **39:** 847–862

Gillespie DT (1977) Exact stochastic simulation of coupled chemical reactions. *J Phys Chem* **81:** 2340–2361

Graf A, Smith AM (2011) Starch and the clock: the dark side of plant productivity. *Trends Plant Sci* **16:** 169–175

Goldberg RN, Bell D, Tewari YB, McLaughlin MA (1991) Thermodynamics of hydrolysis of oligosaccharides. *Biophys Chem* **40:** 69–76

Himmel ME, Ding SY, Johnson DK, Adney WS, Nimlos MR, Brady JW, Foust TD (2007) Biomass recalcitrance: engineering plants and enzymes for biofuels production. *Science* **315:** 804–807

Jencks WP (1997) From chemistry to biochemistry to catalysis to movement. *Annu Rev Biochem* **66:** 1–18

Jones G, Whelan WJ (1969) The action pattern of D-enzyme, a transmaltodextrinylase from potato. *Carbohydr Res* **9:** 483–490

Kakefuda G, Duke SH (1989) Characterization of pea chloroplast D-enzyme (4-α-D-glucanotransferase). *Plant Physiol* **91:** 136–143

Kobayashi S, Ohmae M (2006) Enzymatic polymerization to polysaccharides. *Adv Polym Sci* **194:** 159–210

Landau LD, Lifschitz EM (1979) *Lehrbuch der Theoretischen Physik V: Statistische Physik, Teil 1*. Akademie-Verlag, Berlin: GDR

Lillie SH, Pringle JR (1980) Reserve carbohydrate metabolism in *Saccharomyces cerevisiae*: responses to nutrient limitation. *J Bacteriol* **143:** 1384–1394

Lin T, Preiss J (1988) Characterization of D-enzyme (4-α-Glucanotransferase) in Arabidopsis leaf. *Plant Physiol* **86:** 260–265

Lu Y, Sharkey TD (2004) The role of amylomaltase in maltose metabolism in the cytosol of photosynthetic cells. *Planta* **218:** 466–473

Lu Y, Steichen JM, Yao J, Sharkey T (2006) The role of cytosolic α-glucan phosphorylase in maltose metabolism and the comparison of amylomaltase in Arabidopsis and *Escherichia coli*. *Plant Physiol* **142:** 878–889

Nakatani H (1999) Monte Carlo simulation of 4-α-glucanotransferase reaction. *Biopolymers* **50:** 145–151

Nakatani H (2002) Monte Carlo simulation of hyaluronidase reaction involving hydrolysis, transglycosylation and condensation. *Biochem J* **365:** 701–705

Niittylä T, Messerli G, Trevisan M, Chen J, Smith AM, Zeeman SC (2004) A previously unknown maltose transporter essential for starch degradation in leaves. *Science* **303:** 87–89

Parrou JL, Enjalbert B, Plourde L, Bauche A, Gonzalez B, Francois J (1999) Dynamic responses of reserve carbohydrate metabolism under carbon and nitrogen limitations in *Saccharomyces cerevisiae*. *Yeast* **15:** 191–203

Seeberger PH (2005) Exploring life's sweet spot. *Nature* **437:** 1239

Sharkey TD, Laporte M, Lu Y, Weise S, Weber APM (2004) Engineering plants for elevated CO_2: a relationship between starch degradation and sugar sensing. *Plant Biol* **6:** 280–288

Smith AM, Zeeman SC, Smith SM (2005) Starch degradation. *Annu Rev Plant Biol* **56:** 73–91

Steichen JM, Petty RV, Sharkey TD (2008) Domain characterization of a 4-α-glucanotransferase essential for maltose metabolism in photosynthetic leaves. *J Biol Chem* **283:** 20797–20804

Stitt M, Lunn J, Usadel B (2010) Arabidopsis and primary photosynthetic metabolism—more than the icing on the cake. *Plant J* **61:** 1067–1091

Suganuma T, Setoguchi S, Fujimoto S, Nagahama T (1991) Analysis of the characteristic action of D-enzyme from sweet potato in terms of subsite theory. *Carbohydr Res* **212:** 201–212

Takaha T, Smith SM (1999) The functions of 4-α-glucanotransferases and their use for the production of cyclic glucans. *Biotechnol Genet Eng* **16:** 257–280

Tewari YB, Goldberg RN, Sato M (1997) Thermodynamics of the hydrolysis and cyclization reactions of α-, *β*-, and γ-cyclodextrin. *Carbohydr Res* **301:** 11–22

Thoma JA (1976) Models for depolymerizing enzymes. Application to α-Amylases. *Biopolymers* **15:** 729–746

Thoma JA, Rao GV, Brothers C, Spradlin J, Li LH (1971) Subsite mapping of enzymes. Correlation of product patterns with Michaelis parameters and substrate-induced strain. *J Biol Chem* **246:** 5621–5635

Tobolsky AV (1944) Equilibrium distribution in size for linear polymer molecules. *J Chem Phys* **12:** 402–405

Walker GJ, Whelan WJ (1959) Synthesis of amylose by potato D-enzyme. *Nature* **183:** 46

Warshel A, Sharma PK, Kato M, Xiang Y, Liu H, Olsson MHM (2006) Electrostatic basis for enzyme catalysis. *Chem Rev* **106:** 3210–3235

Wicken JS (1978) The entropy gradient: a heuristic approach to chemical equilibrium. *J Chem Educ* **55:** 701–703

Yoshida Y, Kuroiwa H, Misumi O, Yoshida M, Ohnuma M, Fujiwara T, Yagisawa F, Hirooka S, Imoto Y, Matsushita K, Kawano S, Kuroiwa T (2010) Chloroplasts divide by contraction of a bundle of nanofilaments consisting of polyglucan. *Science* **329:** 949–953

Zeeman SC, Kossmann J, Smith AM (2010) Starch: its metabolism, evolution, and biotechnological modification in plants. *Annu Rev Plant Biol* **61:** 209–234